Minimization of Cogging Torque in Axial-Flux Permanent-Magnet Machines: Design Concepts

M. Aydin[1], Z. Q. Zhu[2], T. A. Lipo[3], *Fellow, IEEE*, and D. Howe[2]

[1]Department of Mechatronics Engineering, Kocaeli University, Kocaeli 41040, Turkey
[2]Department of Electronic and Electrical Engineering, University of Sheffield, Sheffield S1 3JD, U.K.
[3]Department of Electrical and Computer Engineering, University of Wisconsin-Madison, Madison, WI 53706-1691 USA

Various techniques exist for reducing the cogging torque in radial-flux permanent-magnet (RFPM) machines. However, although some of these can be applied to axial-flux PM (AFPM) machines, the additional manufacturing complexity and cost may be prohibitive. Therefore, alternative low-cost techniques are desirable for use in AFPM machines. In this paper, the utility of employing cogging torque minimization techniques that have been developed principally for use in RFPM machines is examined by 3-D finite-element analysis, and several alternative cogging torque minimization techniques for AFPM machines are proposed.

***Index Terms*—Axial flux, cogging torque, permanent magnet, torque ripple.**

I. Introduction

ASSESSING the torque performance of different machine designs remains a challenging task, since not only must the torque density be considered, but also the torque ripple [1]–[5]. The main sources of torque ripple are [1]–[3]: a) cogging; b) pulsewidth modulated (PWM) current harmonics; (c) nonideal back-electromotive force (EMF) waveforms; d) phase commutation events; and e) causes such as dc-link voltage pulsation and inverter dead-time. At high speeds, torque ripple is usually filtered out by the system inertia. However, at low speeds, torque ripple may result in an unacceptable speed variation, vibration, and acoustic noise.

This paper is concerned only with the minimization of cogging torque, since it is often a significant consideration during the design of permanent-magnet (PM) machines. It occurs from the interaction between air-gap permeance harmonics due to stator slotting and magnetomotive force (MMF) harmonics due to the permanent magnets. The investigation is focused on axial-flux PM (AFPM) machines. A variety of techniques exist for reducing the cogging torque of radial-flux PM (RFPM) machines [6]–[27], such as skewing the slots and/or magnets, displacing and shaping the magnets, employing auxiliary slots or teeth, optimizing the magnet pole-arc to pole-pitch ratio, employing a fractional number of slots per pole, and imparting a sinusoidal self-shielding magnetization distribution, etc. These were recently reviewed in [28]. Some of the techniques can be applied directly to AFPM machines [29]–[35]. However, their impact on manufacturing cost may be prohibitive. Consequently, alternative low-cost techniques for use in AFPM machines are desirable. In this paper, the utility of various cogging torque minimization techniques for AFPM machines is examined by 3-D finite-element analysis, and several new approaches are proposed.

Digital Object Identifier 10.1109/TMAG.2007.902818

II. Computation of Cogging Torque

Irrespective of whether the cogging torque waveform is determined analytically or by finite-element analysis (FEA), it can be described by a Fourier series [8]

$$T_{\text{cog}}(\theta_m) = \sum_{k=1}^{\infty} T_k \sin(kN_c\theta_m + \varphi_k) \tag{1}$$

where θ_m is the rotor rotating position, T_k and φ_k are the amplitude and phase of the kth harmonic component, N_c is the least common multiple between the number of rotor poles, $2p$, and the number of stator slots, N_s. When the number of slots per pole is an integer, $N_c = N_s$.

The cogging torque can be computed by finite-element analysis using either Maxwell's stress tensor or the virtual work technique [36]–[40]. Maxwell's stress tensor method has the advantage that each cogging torque calculation only requires a single field computation. However, the achievable accuracy is critically dependent on the discretization and the integration path. On the other hand, the virtual work method is generally easier to implement [36]. However, it requires field calculations at two rotor positions, and the accuracy may be compromised by the numerical error resulting from the difference of two similar large values of magnetic energy. In this paper, the 3-D finite-element software Maxwell is employed to calculate the cogging torque based on the virtual work principle. However, since 3-D modeling is generally required for analyzing the cogging torque in AFPM machines [29]–[35], and this remains relatively time consuming [36], [37], analytical techniques are combined with 3-D finite-element analyses whenever possible in order to simplify the calculation. The effectiveness of this approach has already been demonstrated in [27], [28], [41]–[44]. For example, if one rotor of a double rotor AFPM machine is displaced by an angle Δ relative to the other rotor, the resultant cogging torque

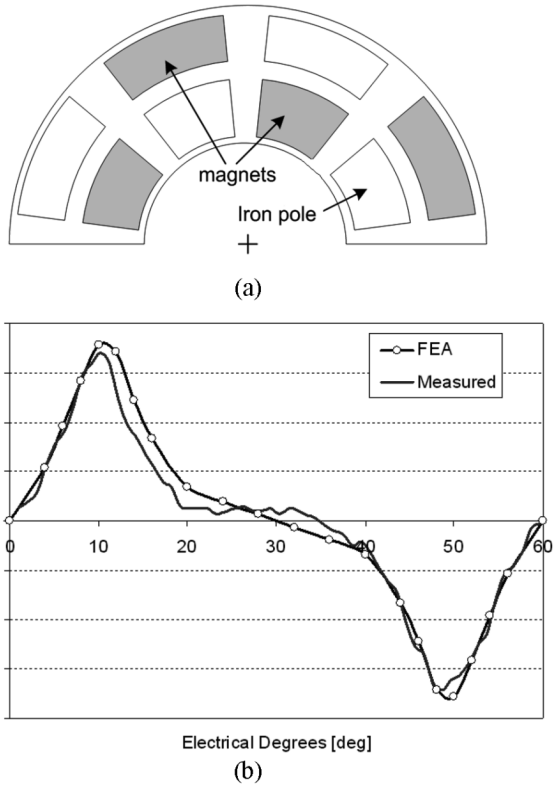

Fig. 1. Comparison of predicted and measured cogging torque for AFPM machine [34].

can be synthesized analytically:

$$T_{\text{cog}}(\theta_m) = \sum_{k=1}^{\infty} T_k \sin(kN_c\theta_m + \varphi_k) + \sum_{k=1}^{\infty} T_k \sin\left[kN_c(\theta_m + \Delta) + \varphi_k\right] = \sum_{k=1}^{\infty} 2T_k \cos\left(kN_c\frac{\Delta}{2}\right) \times \sin\left[kN_c\left(\theta_m + \frac{\Delta}{2}\right) + \varphi_k\right] \quad (2)$$

where T_k is the amplitude of the kth harmonic component of cogging torque due to one rotor.

Hence, the resultant cogging torque is reduced, compared with that which results in an AFPM machine without such a rotor displacement, by the factor

$$\cos\left(kN_c\frac{\Delta}{2}\right) \quad (3)$$

for each harmonic component.

When the permanent magnets are disposed asymmetrically or unequal width magnets are employed, the cogging torque can be similarly synthesized and reduced.

The cogging torque waveform of a double-rotor, single-stator AFPM machine has been calculated by finite-element analysis and validated by measurements [34]. The machine not only had magnets affixed to the rotor surface but also iron pole pieces, in order to increase the flux-weakening capability, as illustrated in Fig. 1(a). However, cogging torque minimization features were not specifically employed because of the cost implications. As will be seen from Fig. 1(b), the predicted and measured results compare favorably.

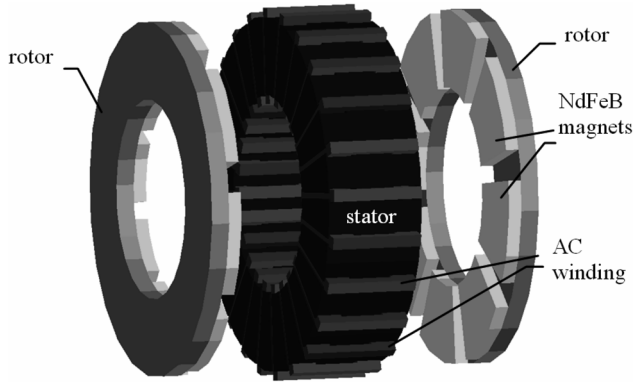

Fig. 2. 8-pole, 24-slot axial-flux surface-mounted magnet machine.

TABLE I
PARAMETERS OF REFERENCE AXIAL-FLUX PM MACHINE

Stator outer diameter	89mm	Pole number	8
Stator inner diameter	50mm	Mechanical airgap	0.8mm
Diameter ratio	0.56	Number of phases	3
Axial thickness of magnets	7.2mm	Number of slots	24
Axial thickness of stator yoke	22mm	Slots / pole / phase	1
Magnet pole-arc/pole-pitch ratio	0.756		

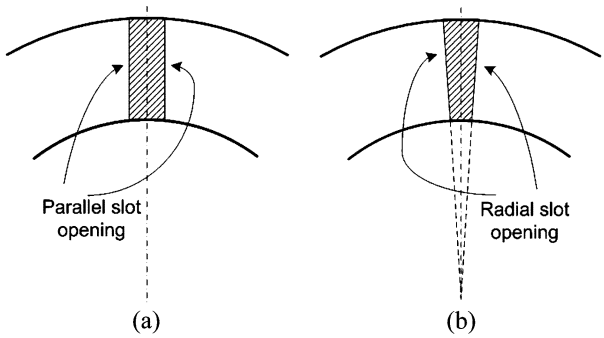

Fig. 3. (a) Parallel and (b) radial slot openings for AFPM machines.

III. PARAMETERS OF AFPM REFERENCE MACHINE

The investigation that is reported in this paper is based on an AFPM machine that consists of a 24-slot stator sandwiched between two 8-pole rotors, as shown in Fig. 2. The stator comprises a tape wound core and a gramme-ring type winding, while the rotor comprises a mild-steel disc and "fan"-shaped surface-mounted magnets. The machine parameters are given in Table I. Parallel stator slot openings (Fig. 3), rather than radial slot openings, are employed to ease manufacture. When the slot openings are parallel, the ratio of the width of the slot openings to the slot-pitch is not constant. As a consequence, the effective cogging torque waveforms at different radii are different. This is in

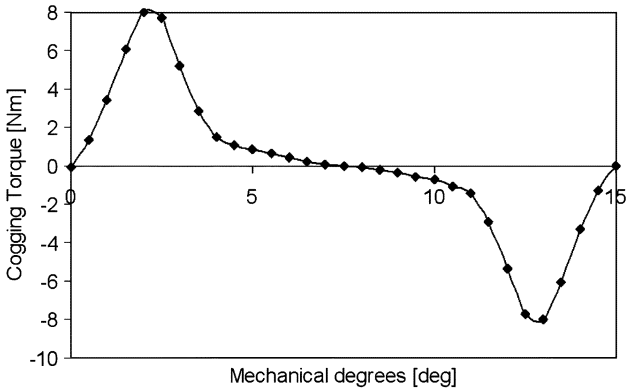

Fig. 4. Cogging torque waveform of reference AFPM machine (Number of finite elements for each torque point: 170 176 tetrahedras, total CPU time: 25 min, Computer used: P4-1.8 MHz PC).

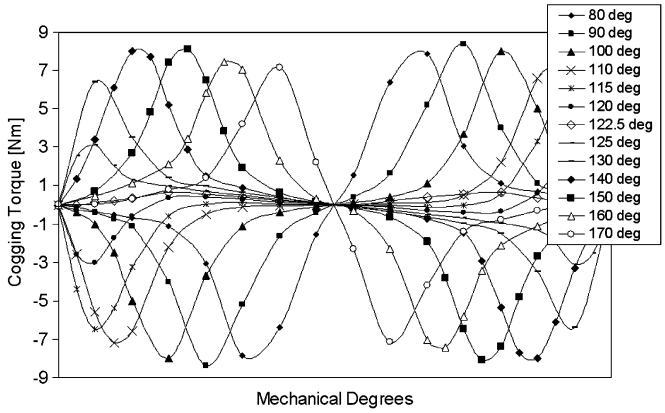

Fig. 5. Variation of one cycle of cogging torque waveform with magnet pole arc, for $\alpha_p = 80$–$170°$elec.

contrast to the cogging torque waveform that results with radial slot openings, for which the ratio of the width of the slot openings to the slot-pitch remains constant with the radius. Therefore, as will be shown later, appropriate design of the slot openings in AFPM machines is one of the key means of cogging torque reduction.

The AFPM machine under consideration has a peak cogging torque of 8.0 Nm, the cogging torque waveform being shown in Fig. 4.

IV. Cogging Torque Minimization

As mentioned in the introduction, numerous techniques exist for minimizing the cogging torque, and these are well documented. However, the majority are used to reduce the cogging torque in RFPM machines. In this section, therefore, cogging torque minimization techniques for AFPM machines will be examined, and additional features that might be incorporated in AFPM machine designs to reduce the cogging torque will be highlighted.

A. Ratio of Stator Slot Number to Rotor Pole Number

In integral slot machines, for which the number of slots per pole is an integer, each rotor magnet has the same position relative to the stator slots. Consequently, the cogging torque components that are produced by all the magnets are in phase, which leads to a high resultant cogging torque. However, in fractional slot machines, for which the number of slots per pole is a non-integer, the rotor magnets have different positions relative to the stator slots, and consequently produce cogging torque components that are out of phase with each other. The resultant cogging torque is, therefore, reduced since some of the cogging components are partially cancelled. In general, it is preferable to employ a slot and pole number combination that has a high least common multiple between the number of slots and the number of poles [8]. However, although fractional slot designs are common for RFPM machines, they are unsuitable for some AFPM machines, such as those having a consequent-pole rotor [34] due to the gramme-ring type (or back-to-back type) winding disposition.

B. Dummy Slots in Stator Teeth

One technique for reducing the cogging torque is to introduce dummy slots in the stator teeth [8], [20], which reduces the amplitude and increases the frequency of the cogging torque. However, a significant disadvantage is that this complicates the manufacturing process and, therefore, increases the cost.

C. Magnet Pole-Arc to Pole-Pitch Ratio

The cogging torque can be minimized by employing an appropriate magnet pole-arc to pole-pitch ratio. Since the cogging torque is produced by the interaction between the edges of the magnet poles and the stator slots, both the magnitude and shape of the cogging torque waveform depend on the magnet pole arc. Reducing the magnet pole-arc to pole-pitch ratio reduces the magnet leakage flux, but it also reduces the magnet flux, and, consequently, the average torque. Hence, a compromise is usually required. In addition, consideration needs to be given to the influence of the magnet pole arc on the back-EMF related torque ripple.

The optimum magnet pole arc, α_p, for minimum cogging torque in RFPM machines [8] also applies to AFPM machines, viz.

$$\alpha_p = \frac{N-k}{N}, \quad k = 1, 2 \ldots N-1 \tag{4}$$

where $N = N_c/2_p$, where p is the number of pole pairs. However, in practice the optimum α_p is slightly larger than that given in (4) due to the influence of interpole flux leakage.

Finite-element predicted cogging torque waveforms of the reference AFPM machine shown in Fig. 2 are shown in Fig. 5 for various magnet pole arcs, while Fig. 6 shows the variation in the peak-to-peak amplitude. It can be seen that when the magnet pole arc is 140°elec. ($\alpha_p = 0.778$), the peak cogging torque is ~51% of the rated torque, while when the magnet pole arc is 122.5°elec. ($\alpha_p = 0.68$), the peak cogging torque is a minimum, and is reduced to ~5% of the rated torque.

D. Conventional Skew: Either Stator Slots or Rotor Magnets

Skewing is one of the simplest, most effective, and common techniques to reduce the cogging torque. It also reduces high

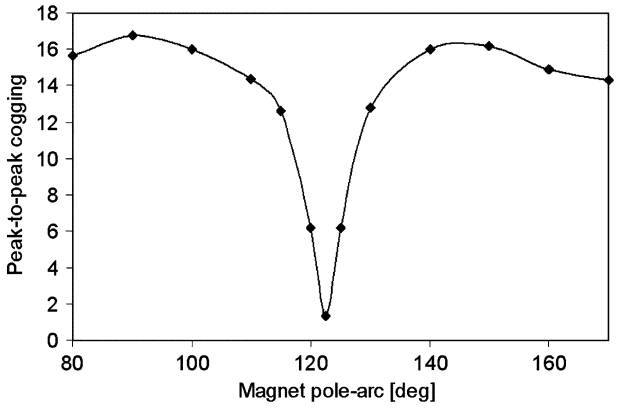

Fig. 6. Variation of peak-to-peak cogging torque of reference machine with magnet pole arc.

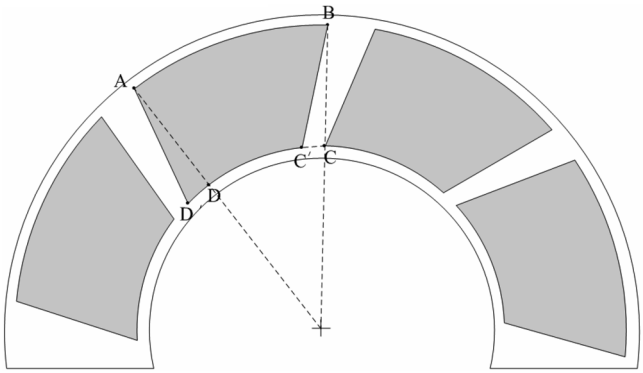

Fig. 7. Skewed magnet AFPM machine rotor. Magnet ABCD is skewed to $\mathrm{ABC'D'}$.

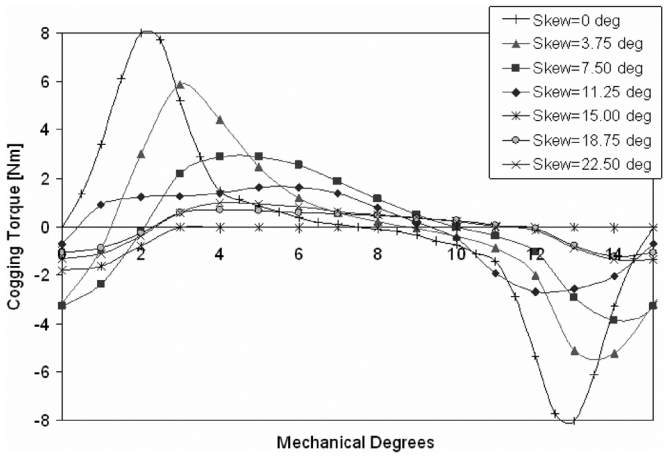

Fig. 8. Variation of cogging torque waveform in AFPM machine with magnet skew angle.

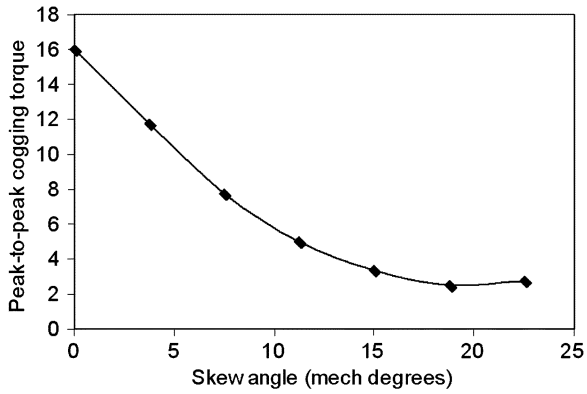

Fig. 9. Variation of peak-to-peak cogging torque with magnet skew angle.

order harmonics in the back-EMF waveform of brushless ac machines. It can be accomplished by skewing either the stator slots or the rotor magnets. If the magnets are skewed by one slot-pitch, the cogging torque effectively becomes zero. However, while skewing the rotor magnets is relatively difficult in RFPM machines, since the shape of the magnets becomes complex, it is relatively easy to skew the magnets in AFPM machines. By way of example, Fig. 7 illustrates both skewed and nonskewed magnets on an AFPM machine rotor, an unskewed magnet being ABCD, whilst the skewed magnet is $\mathrm{ABC'D'}$.

The smallest skew angle for minimizing the cogging torque is [8]

$$\theta_{\text{skew}} = \frac{2\pi}{N_c} \tag{5}$$

for machines having a fractional number of slots per pole, or

$$\theta_{\text{skew}} = \frac{2\pi}{N_s} \tag{6}$$

for machines having an integral number of slots per pole.

As an alternative to skewing the magnets, the stator slots may be skewed, although this increases the leakage inductance, as well as the copper loss (due to the increase in winding length)

In general, as for RFPM machines [8], the peak cogging torque gradually reduces as the skew angle is increased. However, due to magnetic leakage at the inner and outer radii of the magnets in an AFPM machine, the optimal skew angle may not be exactly as given by (5) and (6), while the minimum cogging torque may be not zero. By way of example, Fig. 8 shows the variation of the cogging torque waveform of the reference AFPM machine as the skew angle is varied from a 1/4 slot-pitch to 3/2 slot-pitches, while Fig. 9 shows the variation in the peak-to-peak amplitude of the cogging torque. As can be seen, the peak cogging torque reduces as the skew angle is increased and is a minimum at a skew angle of 18.75°mech.

E. Alternative Magnet Skew Techniques

There are various ways in which the magnets of an AFPM machine may be skewed, as illustrated in Fig. 10. These are investigated in the next four sections.

1) Triangular Skew: Skew may be introduced by bringing the sides of the magnets at the rotor OD closer together while they are moved farther apart at the rotor ID, as shown in Fig. 11, thereby resulting in a triangular shaped airspace between adjacent magnets. The cogging torque waveform has been determined for four different skew angles, δ, with the magnet surface area maintained constant. As can be seen from Fig. 12, a significant reduction in the cogging torque can be achieved as the skew angle, δ, is increased, an 84.3% reduction in the peak cogging torque being achieved when $\delta = 22.5°$mech.

2) Parallel-Sided Magnets: Parallel-sided magnets can also be employed to reduce the cogging torque, since, as illustrated in Fig. 13, this results in skew relative to radial-sided magnets.

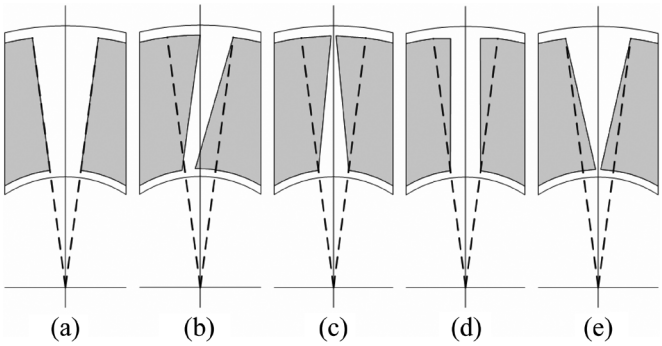

Fig. 10. Various ways of skewing magnet: (a) unskewed, (b) conventional skew, (c) triangular skew, (d) parallel-sided magnets, and (e) trapezoidal skew.

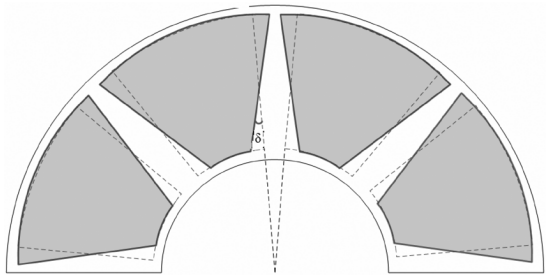

Fig. 11. Triangular skew.

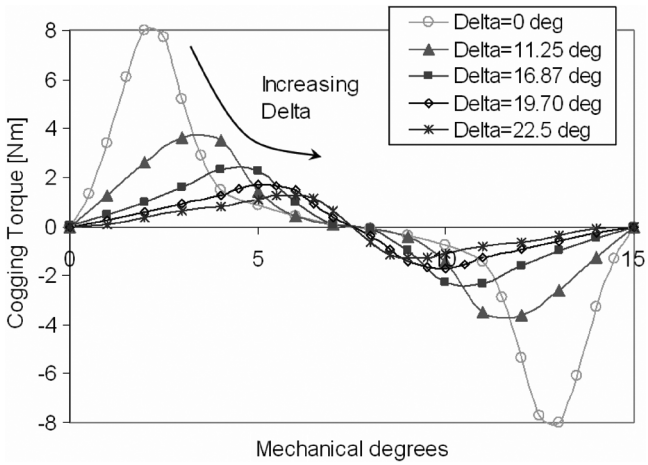

Fig. 12. Variation of cogging torque waveform with angle δ.

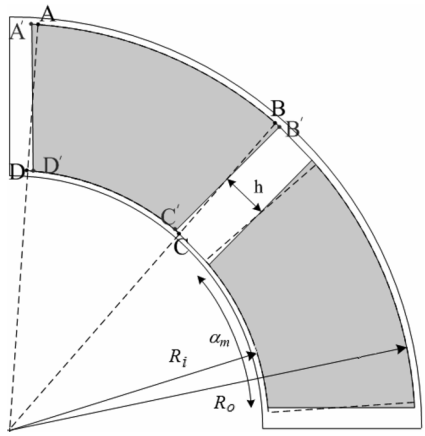

Fig. 13. Comparison of parallel-sided A′B′C′D′ and radial-sided ABCD magnets.

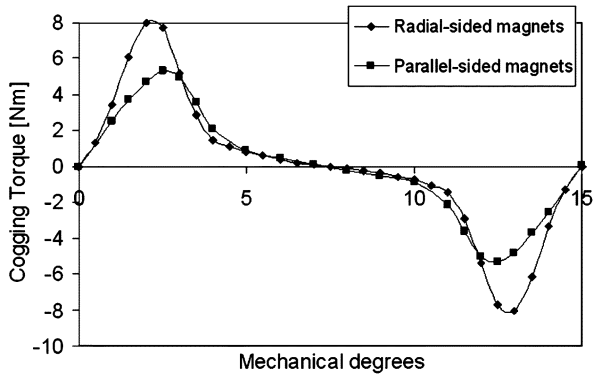

Fig. 14. Comparison of cogging torque waveforms that result with radial- and parallel-sided magnets.

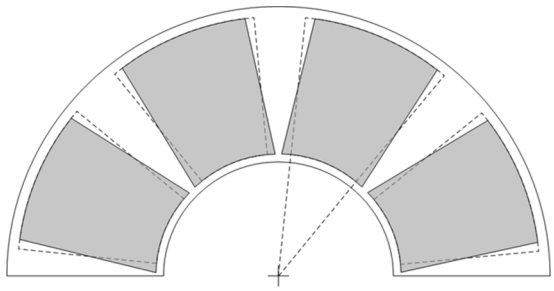

Fig. 15. Trapezoidal skew.

The distance between adjacent magnets is then given approximately by

$$h \approx \frac{\pi}{p}(R_o + R_i)(1 - \alpha_p) \tag{7}$$

where R_i and R_o are the inner and outer radii of the magnet, $\alpha_{\rm p}$ is the pole-arc to pole-pitch ratio, and p is the number of poles. It should be noted that the influence of employing parallel-sided magnets in reducing the cogging torque will be more significant in AFPM machines with a low pole number than those with a high pole number.

Fig. 14 compares the cogging torque waveforms that result with radial- and parallel-sided magnets. It can be seen that the peak cogging torque can be reduced by 34% by employing parallel-sided magnets. The main advantage of this approach that the leakage flux at the outer radius of the magnets is reduced.

3) Trapezoidal Skew: Another way of realizing skew in AFPM machines is illustrated in Fig. 15, in which the magnets are shaped such that their inner edges are closer than the outer edges, so that the ratio of the magnet pole arc to pole pitch at the inner radius is higher than that at the outer radius. This results in a reduction of ~62% in the cogging torque, as shown in Fig. 16. However, one drawback is the fact that the leakage flux at the inner radius of the magnets then increases, which compromises the average torque.

4) Circular Magnets: Circular magnets are also an effective means of introducing skewing in AFPM machines (Fig. 17). To

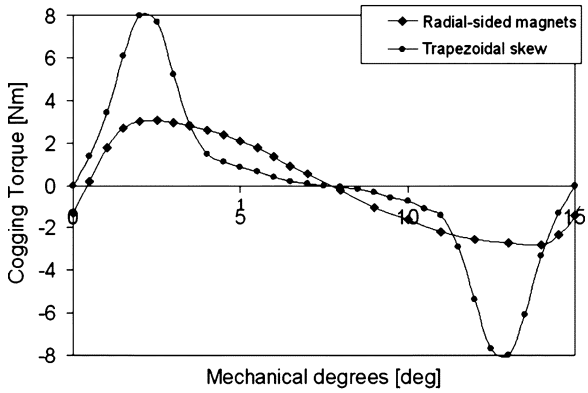

Fig. 16. Comparison of cogging torque waveforms that result with radial-sided magnets and trapezoidal skew.

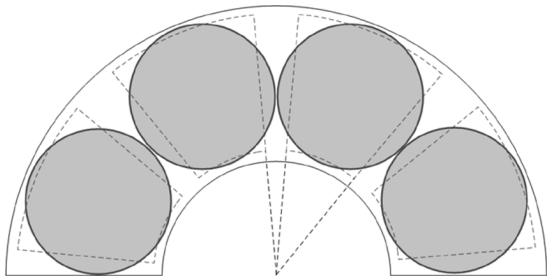

Fig. 17. AFPM machine rotor with circular magnets.

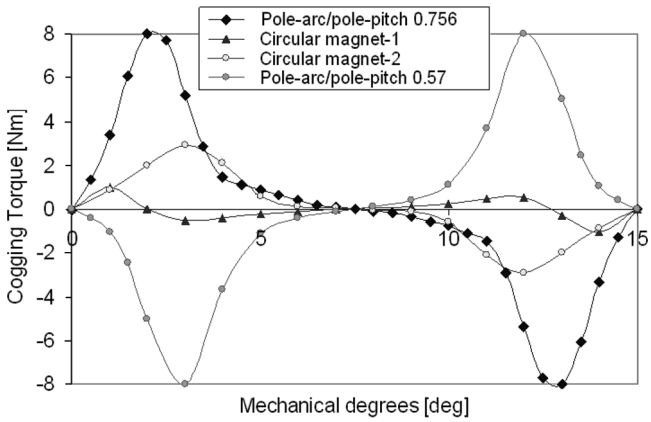

Fig. 18. Comparison of cogging torque waveforms for pole-arc/pole-pitch ratio of 0.756 and 0.57 in reference machine, and with equivalent circular magnets (equivalent pole-arc/pole-pitch ratios in circular magnet-1 and circular magnet-2 are 0.756 and 0.57).

demonstrate this, the cogging torque of the reference AFPM machine has been calculated when the rotor is equipped with circular magnets. Two different diameters of magnet have been considered, their cross-sectional areas being equivalent to magnets having a pole-arc/pole-pitch ratio of 0.756 and 0.57, in the reference machine. As can be seen from Fig. 18, a very significant reduction in the cogging torque can be achieved by employing circular magnets.

5) Dual Skew Magnets: Dual skewed magnets have been successfully employed to reduce the cogging torque in radial-flux PM machines [45] and to eliminate the axial force that generally results with skew. They can readily be employed in AFPM machines, as illustrated in Fig. 19. However, the most likely

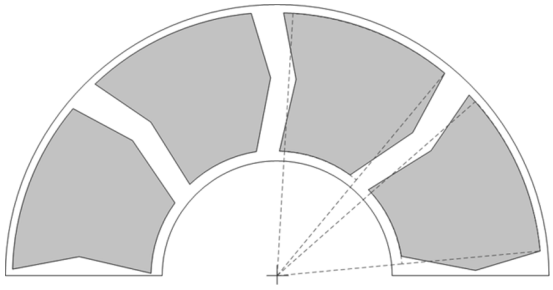

Fig. 19. Dual skew magnets in AFPM machine [45].

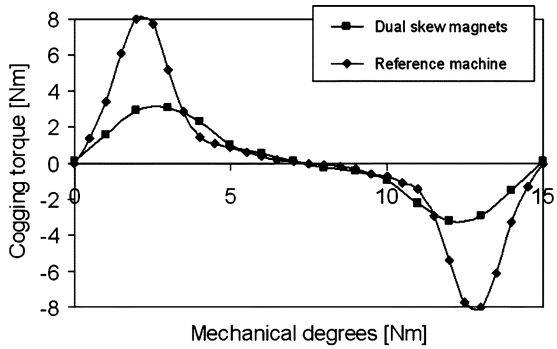

Fig. 20. Comparison of cogging torque waveforms in reference machine and with dual skew magnets.

drawback is the additional complexity and manufacturing cost of such magnets, although the cost of magnets for AFPM machines is usually lower than that for RFPM machines, which are usually radially oriented arc-segments.

The cogging torque, which results when the inner and outer skew angles are identical and the magnet cross-sectional area is the same as that of the magnets in the reference machine, is shown in Fig. 20, for a skew angle of 1/2 slot-pitch. Again, a significant reduction in the cogging torque is achieved.

F. Magnet or Pole Displacement

Another effective technique to minimise the cogging torque is to displace adjacent magnets relative to each other, as illustrated in Fig. 21, both options (a) and (b) being equally effective. However, as the magnets are shifted from their symmetrical positions the leakage flux increases on one side of each magnet and decreases on the other side.

Fig. 22 shows the influence of displacing the magnets with reference to one slot-pitch τ_s on the cogging torque waveform. As will be seen, the cogging torque can be reduced significantly.

G. Variable Magnet Pole Arc

As will be evident from Fig. 5, the phase of the cogging torque waveform changes as the magnet pole arc is varied. Hence, another method of reducing the cogging torque is to employ different magnet pole arcs for adjacent magnets, as illustrated in Fig. 23 such that the phase difference between the associated cogging torques results in a smaller net cogging torque [32], [34], although two different sized magnets are required.

Fig. 24 shows the influence of varying the pole arc of alternate magnets in the reference AFPM machine, with the other magnets having the original pole-arc to pole-pitch ratio of $\tau_m/\tau_p =$

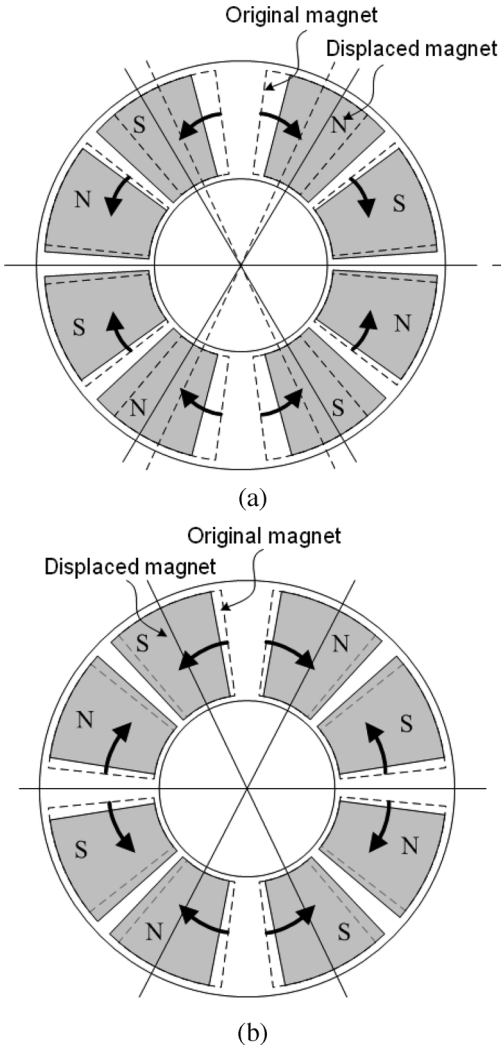

Fig. 21. Options for displacing magnets in AFPM machines.

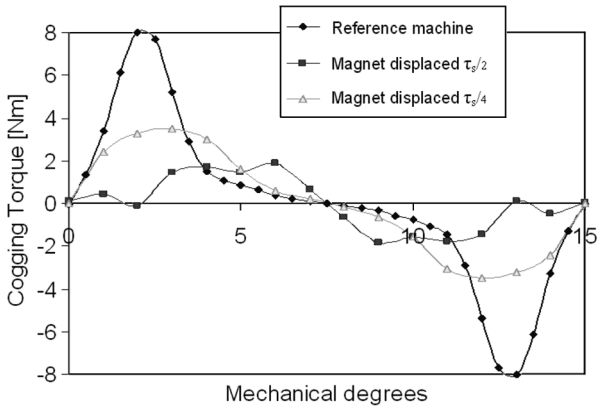

Fig. 22. Influence of displacing magnets on cogging torque of reference machine.

0.756, i.e., $\sim 110°$elec. As will be seen, the peak cogging torque is a maximum when the magnet pole-arc to pole-pitch ratio $\tau_c/\tau_p = 0.611$, and is minimum when the pole-arc to pole-pitch ratio $\tau_m/\tau_p = 0.778$, i.e., $\sim 140°$elec., after which it increases as the pole arc is further increased.

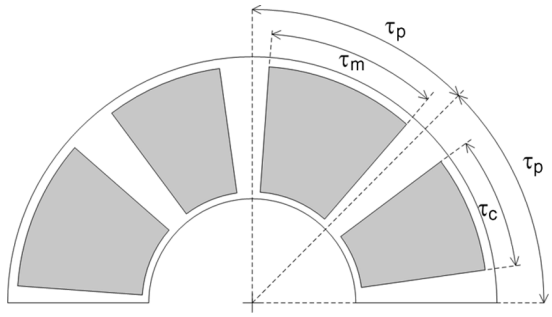

Fig. 23. Rotor equipped with two different magnet pole arcs.

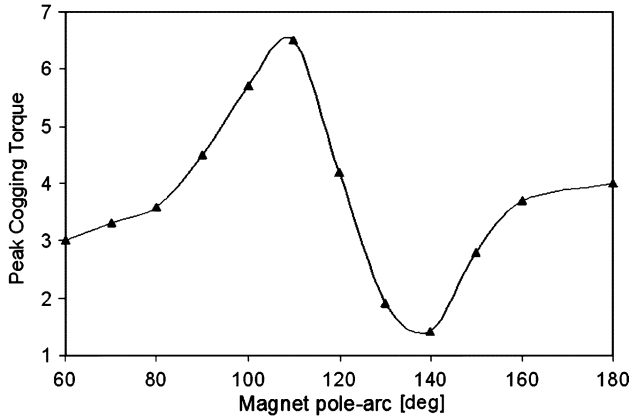

Fig. 24. Variation of peak cogging torque when alternate magnet pole arcs $= 110°$elec. and pole arc of other magnets is varied.

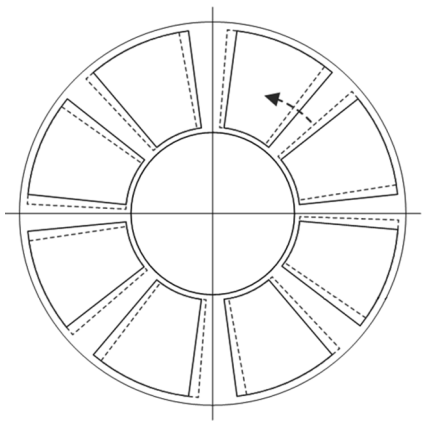

Fig. 25. AFPM machine with two rotors displaced relative to each other.

H. Circumferential Displacement of Rotor/Stator

The cogging torque in a double air-gap AFPM machine results from the superposition of the cogging torque waveforms associated with each air gap. The resultant cogging torque can, therefore, be reduced by circumferentially changing the relative phase of the two rotors of a double-rotor, single-stator AFPM machine or the two stators of a double-stator, single-rotor AFPM machine, as illustrated in Fig. 25.

Cogging torque waveforms that result with various rotor displacements (from 1.5°mech. to 11.5°mech.) are shown in Fig. 26, which also includes the cogging torque waveform of the reference machine. The corresponding variation of the peak cogging torque with the rotor displacement is shown in

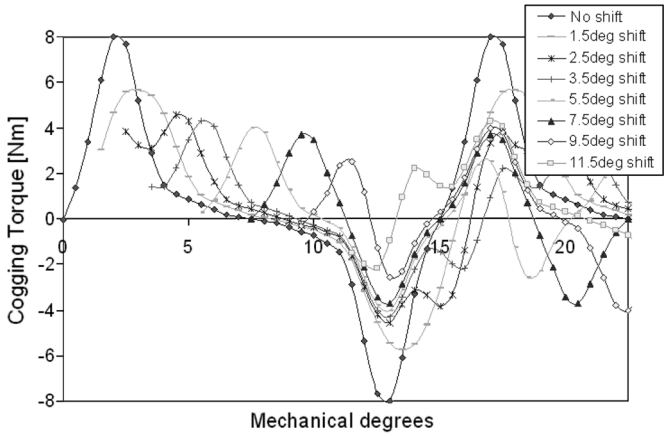

Fig. 26. Variation of cogging torque waveform with rotor displacement.

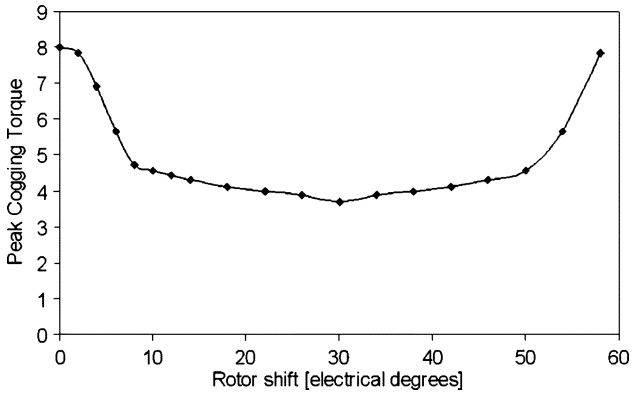

Fig. 27. Variation of peak cogging torque with rotor displacement.

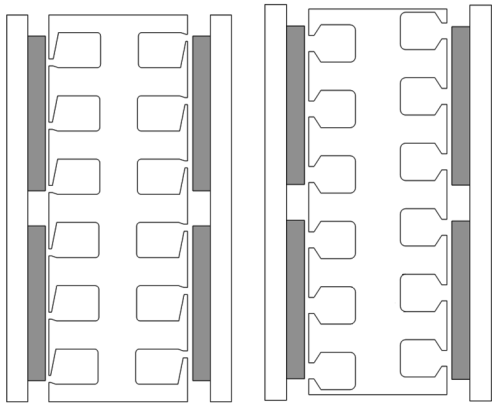

Fig. 28. Displaced stator slot openings and slots. (a) Displaced slot openings. (b) Displaced slots.

Fig. 27, minimum cogging being achieved with a 1/2 slot-pitch (30°elec.).

I. Displaced Slots and Slot Openings

Another approach for reducing the cogging torque is to employ a different stator design such that either the stator slot openings, Fig. 28(a) [35], or the stator slots, Fig. 28(b) [34], on one side can be displaced relative to those on the other side. For example, if the slot openings are displaced by a 1/2 slot-pitch, as shown in Fig. 28(a), the cogging torque waveform associated with each air gap will be phase shifted by 180°elec., so that the resultant cogging torque frequency is doubled and the amplitude is reduced significantly. This will be evident from Fig. 29, which shows that the peak-to-peak cogging torque is decreased by ∼25% when the stator slot openings are displaced by a 1/2 slot-pitch.

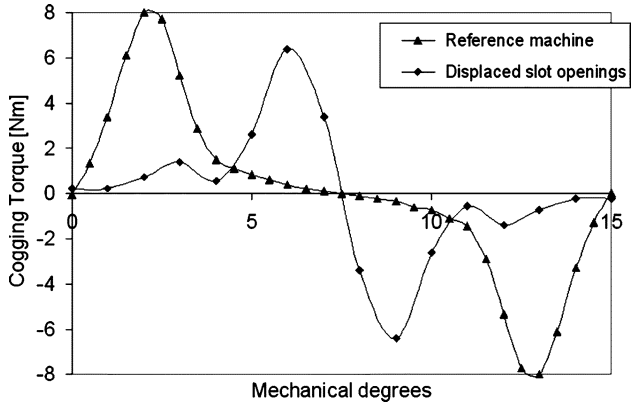

Fig. 29. Comparison of cogging torque waveforms with/without displaced slot openings.

V. Conclusion

Various techniques for minimizing the cogging torque in AFPM machines have been investigated. A double-rotor, single-stator AFPM machine has been used as a reference machine, and the effectiveness of the techniques have been examined by 3-D finite-element analysis.

It has been shown that, similar to RFPM machines, an optimal ratio of magnet pole arc to pole pitch exists for AFPM machines for minimum cogging torque. The combination of stator slot number and pole number affects the cogging torque significantly, and should be selected to make their least common multiple as high as possible. Although the use of a fractional number of slots per pole is advantageous for low cogging torque, and is commonly used for RFPM machines, it should be avoided when a consequent-pole rotor and gramme-ring type stator winding are employed in AFPM machines. The cogging torque can also be reduced by appropriate choice of magnet pole-arc to pole-pitch ratio, but a residual cogging torque usually remains.

As shown in the paper, skewing is very effective in minimizing cogging and can be achieved in several ways in AFPM machines. It has also been shown that in a double air-gap AFPM machine, displacing the stators of a double-stator machine or the rotors of a double-rotor machine relative to each other, or displacing the stator slots or slot openings, is also effective. However, one of the possible drawbacks associated with such features is that the back-EMF waveform becomes more sinusoidal, which may result in the torque ripple in brushless dc drives, but it is advantageous for brushless ac drives. In addition, the back-EMF, and consequently the average torque, will be reduced slightly.

Acknowledgment

The authors are indebted to Ansoft Corp. for providing the finite-element software that has been used in this study.

REFERENCES

[1] J. D. L. Ree and N. Boules, "Torque production in permanent-magnet synchronous motors," *IEEE Trans. Ind. Appl.*, vol. 25, no. 1, pp. 107–112, Jan./Feb. 1989.

[2] T. M. Jahns and W. L. Soong, "Pulsating torque minimization techniques for permanent magnet ac motor drives: A review," *IEEE Trans. Ind. Electron.*, vol. 43, no. 2, pp. 321–330, Apr. 1996.

[3] C. Studer, A. Keyhani, T. Sebastian, and S. K. Murthy, "Study in cogging torque in permanent magnet machines," in *IEEE Ind. Applications Soc. Annu. Meeting*, New Orleans, LA, 1997, pp. 42–49.

[4] D. C. Hanselman, "Effect of skew, pole count and slot count on brushless motor radial force, cogging torque and back EMF," *Inst. Elect. Eng. Proc.—Elect. Power Appl.*, vol. 144, no. 5, pp. 325–330, Sep. 1997.

[5] M. S. Islam, S. Mir, and T. Sebastian, "Issues in reducing the cogging torque of mass-produced permanent-magnet brushless DC motor," *IEEE Trans. Ind. Appl.*, vol. 40, no. 3, pp. 813–820, May–Jun. 2004.

[6] J. A. Wagner, "Numerical analysis of cogging torque in a brushless DC machine," in *IEEE Industry Applications Soc. Annu. Meeting*, 1975, pp. 669–673.

[7] T. Li and G. Slemon, "Reduction of cogging torque in PM motors," *IEEE Trans. Magn.*, vol. 24, no. 6, pp. 2901–2903, Nov. 1988.

[8] Z. Q. Zhu and D. Howe, "Influence of design parameters on cogging torque in permanent magnet machines," *IEEE Trans. Energy Convers.*, vol. 15, no. 4, pp. 407–412, Dec. 2000.

[9] N. Bianchi and S. Bolognani, "Design techniques for reducing the cogging torque in surface-mounted PM motors," *IEEE Trans. Ind. Appl.*, vol. 38, no. 5, pp. 1259–1265, Sep./Oct. 2002.

[10] K. H. Kim, D. J. Sim, and J. S. Won, "Analysis of skew effects on cogging torque and BEMF for BLDCM," in *IEEE Industry Applications Soc. Annu. Meeting*, 1991, pp. 191–197.

[11] R. P. Deodhar, D. A. Staton, T. M. Jahns, and T. J. E. Miller, "Prediction of cogging torque using the flux-MMF diagram technique," *IEEE Trans. Ind. Appl.*, vol. 32, no. 3, pp. 569–576, May–Jun. 1996.

[12] J. M. Kauffmqnn, A. Miraoui, and L. Kong, "Irregular shifting of permanent magnet to reduce the cogging torque of a brushless motor," in *IEEE Industry Applications Soc. Annu. Meeting*, 1991, pp. 191–197.

[13] Z. Q. Zhu and D. Howe, "Analytical prediction of the cogging torque in radial-field permanent magnet brushless motors," *IEEE Trans. Magn.*, vol. 28, no. 2, pp. 1080–1083, Mar. 1992.

[14] T. Ishikawa and G. Slemon, "A method of reducing ripple torque in permanent magnet motors without skewing," *IEEE Trans. Magn.*, vol. 29, no. 2, pp. 2028–2031, Mar. 1993.

[15] A. Keyhani, C. Studer, T. Sebastian, and S. K. Murthy, "Study of cogging torque in permanent magnet machines," *Elect. Mach. Power Syst.*, vol. 27, pp. 665–678, 1999.

[16] C. Breton, J. Bartolome, J. Benito, G. Tassinario, I. Flotats, C. W. Lu, and B. J. Chalmers, "Influence of machine symmetry on reduction of cogging torque in permanent magnet brushless motors," *IEEE Trans. Magn.*, vol. 36, no. 5, pp. 3819–3823, Sep. 2000.

[17] S. K. Chang, S. Y. Hee, W. N. Ki, and S. C. Hong, "Magnetic pole shape optimization of permanent magnet motor for reduction of cogging torque," *IEEE Trans. Magn.*, vol. 33, no. 2, pp. 1822–1827, Mar. 1997.

[18] C. S. Koh, H. Yoon, K. Namn, and H. Choi, "Magnetic pole shape optimization of permanent magnet machine for reduction of cogging torque," *IEEE Trans. Magn.*, vol. 33, no. 2, pp. 1822–1827, Mar. 1997.

[19] M. Goto and K. Kobayashi, "An analysis of the cogging torque of a DC motor and a new technique of reducing the cogging torque," *Elect. Eng. Jpn.*, vol. 103, no. 5, pp. 113–120, 1983.

[20] K. Kobayashi and M. Goto, "A brushless DC motor of a new structure with reduced torque fluctuations," *Elect. Eng. Jpn.*, vol. 105, no. 3, pp. 104–112, 1985.

[21] B. Ackermann, J. H. H. Janssen, R. Sottek, and R. I. Van Steen, "New technique for reducing cogging torque in class of brushless motors," *Inst. Elect. Eng. Proc.—Elect. Power Appl.*, vol. 139, no. 4, pp. 315–320, 1992.

[22] J. R. Hendershot and T. J. E. Miller, *Design of Brushless Permanent Magnet Motors*. Oxford, U.K.: Magna Physics & Clarendon Press, 1994.

[23] C. C. Hwang, S. B. John, and S. S. Wu, "Reduction of cogging torque in spindle motors for CD-ROM drive," *IEEE Trans. Magn.*, vol. 34, no. 2, pp. 468–470, Mar. 1998.

[24] Y. D. Yao, D. R. Huang, J. C. Wang, S. H. Liou, S. J. Wang, T. F. Ying, and D. Y. Chiang, "Simulation study of the reduction of cogging torque in permanent magnet machines," *IEEE Trans. Magn.*, vol. 33, no. 5, pp. 4095–4097, Sep. 1997.

[25] J. Hur and D. Hyun, "A method for reduction of cogging torque in brushless DC machine considering the distribution of magnetization by 3DEMCN," *IEEE Trans. Magn.*, vol. 34, no. 5, pp. 3532–3535, Sep. 1998.

[26] Y. Pang, Z. Q. Zhu, and D. Howe, "Self-shielding magnetised vs. shaped parallel magnetised PM brushless ac motors," *Kor. IEE Int. Trans. Elect. Mach. Energy Convers. Syst.*, vol. 5-B, no. 1, pp. 13–19, 2005.

[27] Z. Q. Zhu, S. Ruangsinchaiwanich, D. Ishak, and D. Howe, "Analysis of cogging torque in brushless machines having non-uniformly distributed stator slots and stepped rotor magnets," *IEEE Trans. Magn.*, vol. 41, no. 10, pp. 3910–3912, Oct. 2005.

[28] Z. Q. Zhu, S. Ruangsinchaiwanich, and D. Howe, "Synthesis of cogging torque from a single stator slot in permanent magnet machines," *IEEE Trans. Ind. Appl.*, vol. 42, no. 3, pp. 650–657, May–Jun. 2006.

[29] G. Bakarat, T. El-Meslouhi, and B. Dakyo, "Analysis of the cogging torque behavior of a two-phase axial-flux permanent magnet synchronous machine," *IEEE Trans. Magn.*, vol. 37, no. 4, pp. 2803–2805, Jul. 2001.

[30] F. Caricchi, F. Giulii Capponi, F. Crescimbini, and L. Solero, "Experimental study on reducing cogging torque and core power loss in axial-flux permanent-magnet machines with slotted winding," in *IEEE Industry Applications Soc. Annu. Meeting*, 2002, pp. 1295–1302.

[31] E. Muljadi and J. Green, "Cogging torque reduction in a permanent magnet wind turbine generator," presented at the 21th Amer. Soc. Mechanical Engineers Wind Energy Symp., Reno, NV, 2002.

[32] M. Aydin, R. Qu, and T. A. Lipo, "Cogging torque minimization technique for multiple-rotor, axial-flux, surface-mounted-PM machines: Alternating magnet pole-arcs in facing rotors," in *IEEE Industry Applications Soc. Annu. Meeting*, 2003, pp. 555–561.

[33] A. Letelier, J. A. Tapia, R. Wallace, and A. Valenzuela, "Cogging torque reduction in an axial-flux PM machine with extended speed range," in *Proc. IEEE Int. Electrical Machines and Drive Conf.*, 2005, pp. 1261–1267.

[34] M. Aydin, "Axial-flux surface mounted permanent magnet disc machines for smooth torque traction drive applications," Ph.D. thesis, Univ. Wisconsin, Madison, 2004.

[35] R. Qu and T. A. Lipo, "Dual-rotor, radial-flux, toroidally wound, permanent-magnet machines," *IEEE Trans. Ind. Appl.*, vol. 39, no. 6, pp. 1665–1673, May–Jun. 2003.

[36] S. J. Salon, *Finite Element Analysis of Electrical Machines*. Norwell, MA: Kluwer, 1995.

[37] J. L. Coulomb, "A methodology for the determination of global electromechanical quantities from a finite element analysis and its application to the evaluation of magnetic forces, torques and stiffness," *IEEE Trans. Magn.*, vol. 19, no. 6, pp. 2514–2519, Nov. 1983.

[38] D. Howe and Z. Q. Zhu, "The influence of finite element discretisation on the prediction of cogging torque in permanent magnet excited machines," *IEEE Trans. Magn.*, vol. 28, no. 2, pp. 1080–1083, Mar. 1992.

[39] C. M. Chao, S. J. Wang, C. P. Liao, D. R. Huang, and T. F. Ying, "Torque and cogging torque in sandwich type CD-ROM spindle machine," *IEEE Trans. Magn.*, vol. 34, no. 2, pp. 471–473, Mar. 1998.

[40] Y. Kawase, T. Yamaguchi, and Y. Hayashi, "Analysis of cogging torque of permanent magnet machine by 3-D finite element method," *IEEE Trans. Magn.*, vol. 31, no. 3, pp. 2044–2047, May 1995.

[41] Z. Q. Zhu, P. J. Hor, D. Howe, and J. Rees-Jones, "Calculation of cogging force in a novel slotted linear tubular brushless permanent magnet machine," *IEEE Trans. Magn.*, vol. 33, no. 5, pp. 4098–4100, Sep. 1997.

[42] P. J. Hor, Z. Q. Zhu, and D. Howe, "Minimization of cogging force in a novel slotted linear brushless permanent magnet machine," *IEEE Trans. Magn.*, vol. 34, no. 5, pp. 3544–3547, Sep. 1998.

[43] Z. Q. Zhu, Z. P. Xia, D. Howe, and P. H. Mellor, "Reduction of cogging force in linear permanent magnet machines," *Proc. Inst. Elect. Eng.—Elect. Power Appl.*, vol. 144, no. 4, pp. 277–282, 1997.

[44] Z. Q. Zhu, S. Ruangsinchaiwanich, Y. Chen, and D. Howe, "Evaluation of superimposition technique for calculating cogging torque in permanent magnet brushless machines," *IEEE Trans. Magn.*, vol. 42, no. 3, pp. 1597–1603, Mar. 2006.

[45] F. Jurisch, "Shell-shaped magnet," U. S. Patent US24028945A1, 2004.

Manuscript received October 5, 2006; revised June 16, 2007. Corresponding author: Z. Q. Zhu (e-mail: z.q.zhu@sheffield.ac.uk).